Available online at www.sciencedirect.com
SCIENCE DIRECT
ELSEVIER
Icarus 178 (2005) 312–326
ICARUS
www.elsevier.com/locate/icarus

Cassini UVIS observations of Jupiter's auroral variability

Wayne R. Pryor [a,*], A. Ian F. Stewart [b], Larry W. Esposito [b], William E. McClintock [b], Joshua E. Colwell [b], Alain J. Jouchoux [b], Andrew J. Steffl [b], Donald E. Shemansky [c], Joseph M. Ajello [d], Robert A. West [d], Candace J. Hansen [d], Bruce T. Tsurutani [d], William S. Kurth [e], George B. Hospodarsky [e], Donald A. Gurnett [e], Kenneth C. Hansen [f], J. Hunter Waite Jr. [f], Frank J. Crary [g], David T. Young [g], Norbert Krupp [h], John T. Clarke [i], Denis Grodent [j], Michele K. Dougherty [k]

[a] *Central Arizona College, 8470 N. Overfield Road, Coolidge, AZ 85228, USA*
[b] *Laboratory for Atmospheric and Space Physics, University of Colorado, Boulder, CO, USA*
[c] *University of Southern California, Los Angeles, CA, USA*
[d] *Jet Propulsion Laboratory, Pasadena, CA, USA*
[e] *University of Iowa, Iowa City, IA, USA*
[f] *University of Michigan, Ann Arbor, MI, USA*
[g] *Southwest Research Institute, San Antonio, TX, USA*
[h] *Max-Planck-Institut für Sonnensystemforschung, Katlenburg-Lindau, Germany*
[i] *Boston University, Boston, MA, USA*
[j] *University of Liege, Liege, Belgium*
[k] *University College, London, UK*

Received 12 October 2004; revised 16 April 2005

Available online 24 August 2005

Abstract

The Cassini spacecraft Ultraviolet Imaging Spectrograph (UVIS) obtained observations of Jupiter's auroral emissions in H_2 band systems and H Lyman-α from day 275 of 2000 (October 1), to day 81 of 2001 (March 22). Much of the globally integrated auroral variability measured with UVIS can be explained simply in terms of the rotation of Jupiter's main auroral arcs with the planet. These arcs were also imaged by the Space Telescope Imaging Spectrograph (STIS) on Hubble Space Telescope (HST). However, several brightening events were seen by UVIS in which the global auroral output increased by a factor of 2–4. These events persisted over a number of hours and in one case can clearly be tied to a large solar coronal mass ejection event. The auroral UV emissions from these bursts also correspond to hectometric radio emission (0.5–16 MHz) increases reported by the Galileo Plasma Wave Spectrometer (PWS) and Cassini Radio and Plasma Wave Spectrometer (RPWS) experiments. In general, the hectometric radio data vary differently with longitude than the UV data because of radio wave beaming effects. The 2 largest events in the UVIS data were on 2000 day 280 (October 6) and on 2000 days 325–326 (November 20–21). The global brightening events on November 20–21 are compared with corresponding data on the interplanetary magnetic field, solar wind conditions, and energetic particle environment. ACE (Advanced Composition Explorer) solar wind data was numerically propagated from the Earth to Jupiter with an MHD code and compared to the observed event. A second class of brief auroral brightening events seen in HST (and probably UVIS) data that last for ~2 min is associated with auroral flares inside the main auroral ovals. On January 8, 2001, from 18:45–19:35 UT UVIS H_2 band emissions from the north polar region varied quasiperiodically. The varying emissions, probably due to auroral flares inside the main auroral oval, are correlated with low-frequency quasiperiodic radio bursts in the 0.6–5 kHz Galileo PWS data.
© 2005 Elsevier Inc. All rights reserved.

* Corresponding author.
E-mail address: wayne_pryor@centralaz.edu (W.R. Pryor).

0019-1035/$ – see front matter © 2005 Elsevier Inc. All rights reserved.
doi:10.1016/j.icarus.2005.05.021

Keywords: Auroras; Jupiter; Solar wind; Ultraviolet

1. Introduction

The Galileo spacecraft orbited Jupiter from December 1995 to September 2003. The Cassini spacecraft (Matson et al., 2002) flew past Jupiter on December 30, 2000, at an altitude of 9.7 million kilometers on its way to Saturn, providing an opportunity for several months of joint observations of the Jupiter system by the two spacecraft, by the Hubble Space Telescope, and by other facilities. The encounter featured Cassini solar wind monitoring by CAPS (Cassini Plasma Spectrometer, Young et al., 2004) and MAG (Magnetometer, Dougherty et al., 2004), and auroral observations by UVIS (Esposito et al., 2004) mostly from outside the magnetosphere, while the Galileo EPD (Energetic Particle Detector, Williams et al., 1992) was making energetic particle measurements relevant to auroral processes from inside the magnetosphere. A *Nature* special issue described initial results from the joint observation campaign (Hill, 2002; Gurnett et al., 2002; Bolton et al., 2002; Kurth et al., 2002; Krimigis et al., 2002; Clarke et al., 2002; Gladstone et al., 2002; Mauk et al., 2002). Radio emissions observed by the Cassini RPWS (Gurnett et al., 2004) and Galileo PWS (Gurnett et al., 1992) experiments were at times closely linked to auroral emissions observed by UVIS, as will be detailed here (Gurnett et al., 2002, presented a related report from the Cassini RPWS point of view).

This paper focuses on Cassini UVIS observations of Jupiter's auroras during this campaign, including initial auroral spectroscopy, detection of UV auroral brightening events on both long and short timescales, and comparisons with radio emissions, solar wind conditions, and the energetic particle environment. Conclusions will be drawn about large-scale auroral storms and their relationship to coronal mass ejection events, and about brief UV bursts inside the auroral ovals and their relationship to radio bursts over the poles near the magnetopause.

The Cassini UVIS instrument and its objectives are described in Esposito et al. (2004). The current paper focuses on UVIS observations by the Extreme Ultraviolet (EUV) and Far Ultraviolet (FUV) spectrograph channels. Each channel has 3 selectable slits that admit light that is dispersed by a holographic toroidal grating and imaged onto Coded Anode Converter (CODACON) solar-blind microchannel plate detectors with 1024 spectral by 64 spatial pixels. The EUV channel covers 56.3–118.2 nm with 0.3–1.9-nm resolution, depending on the chosen slit, while the FUV channel covers 111.5–191.2 nm with 0.3–2.5-nm resolution.

2. Auroral spectroscopy

Jupiter's intense polar auroral spectrum in the EUV and FUV spectral regions consists primarily of H_2 band emissions and the H Lyman-α line produced primarily by energetic electron precipitation. These auroral emissions have been discussed by many authors, and were reviewed by Bhardwaj and Gladstone, 2000. Cassini UVIS spectra improve on many earlier data sets, because of the extensive simultaneous EUV and FUV measurements with good counting statistics, and because both day and nightside observations were obtained. The EUV channel observes emissions from low-energy (0.1–3 keV) precipitating particle "soft" auroras at a column density in H_2 of perhaps 10^{16} cm^{-2}. This is well above the methane homopause. The EUV depth of observation is limited by self-absorption in H_2 gas (Ajello et al., 2001). The FUV channel observes longer wavelengths where H_2 self-absorption does not occur, and observes a wide range of auroral altitudes. At least some auroral emission occurs below the methane homopause, as characteristic absorptions due to CH_4, C_2H_6, and C_2H_2 are evident in FUV spectra (e.g., Galileo spectra described by Ajello et al., 1998, 2001). The main aurora is thought to occur at an H_2 column of 10^{20}–10^{21} cm^{-2}, near ∼245 km above the 1-bar pressure level (Vasavada et al., 1999).

Fig. 1 shows sample EUV and FUV UVIS spatially-resolved spectra. Fig. 2 shows a spatially summed auroral spectrum, compared to the electron impact spectrum of H_2 gas. The FUV data are quite similar to the lab spectrum, while the EUV data show more differences due to self-absorption in H_2 gas. Short-wavelength differences in the FUV between the lab data and the Jupiter data can be modeled by adding hydrocarbon absorbers above the auroral emission, such as CH_4 and C_2H_2. Fig. 3 shows a full spectral model applied to UVIS spectra, based on models developed to fit Galileo and Hopkins Ultraviolet Telescope (HUT) spectra by Ajello et al. (2001). An optically thin auroral spectral component due to soft electrons is required in the fit to this spectrum at EUV wavelengths. A recent electron transport model by Grodent et al. (2001) with a flux of weak (0.1 keV), soft (∼3 keV) and hard (15 keV) electrons is capable of modeling Cassini (Ajello et al., 2005), Far-Ultraviolet Spectrographic Explorer (FUSE) and HUT Jupiter auroral observations (Grodent et al., 2003; Gustin et al., 2002, 2004). Thus, there is evidence in auroral spectra from Galileo, HUT, FUSE and now Cassini for significant emission at high altitudes from a soft electron source, in addition to the main auroral component deep in the atmosphere.

3. UVIS auroral time-series

The simplest UVIS data sets to work with are those obtained early and late in the Cassini flyby when Jupiter was spatially unresolved. We have used these to address the issues of global auroral output and its variability. (The rather

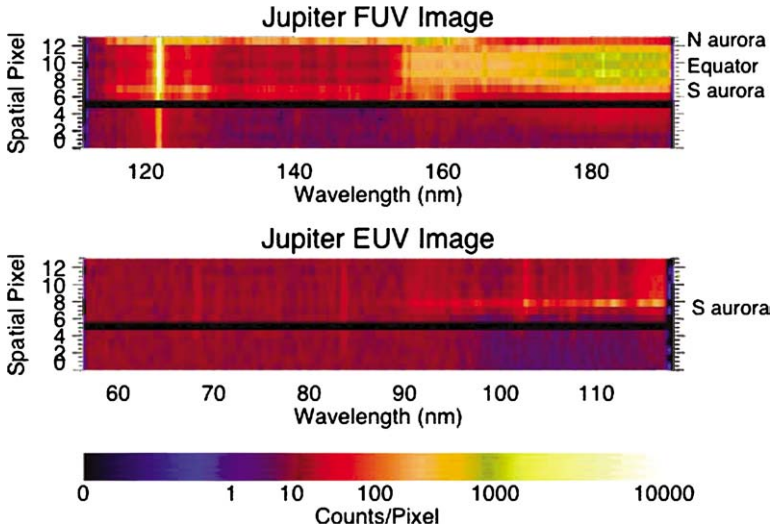

Fig. 1. Sample summed UVIS Jupiter dayside spectral image from 2000 days 345–346; 14 1-mrad spatial pixels are shown on the vertical axis; 1024 wavelength pixels are shown on the horizontal axis (in nm). The counts/pixel are indicated by color. H_2 auroral band emissions from both poles are seen in the FUV below 165 nm. The disk scattered Rayleigh scattered emissions are seen at the longest wavelengths near 180 nm; note that the equator is relatively dark. The EUV channel observed the S pole H_2 band emissions in spatial pixels 7 and 8. Spatial pixel 5 was not working due to a temporary software problem. Torus emission lines are seen, including ionized sulfur at 68.5 and ionized oxygen at 83.4 nm. H Lyman-α emission is seen at 121.6 nm both on and off the planet.

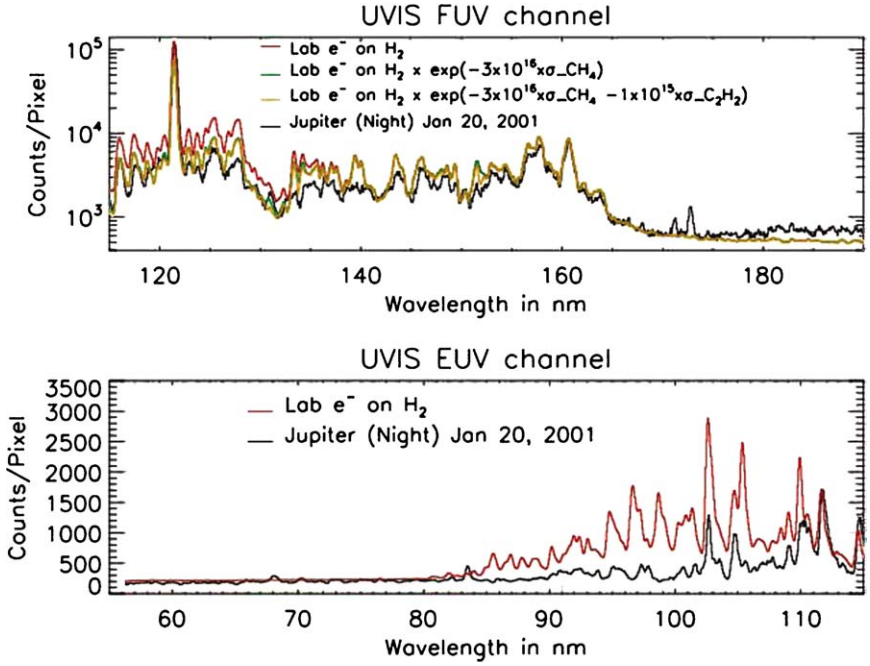

Fig. 2. Summed UVIS FUV H_2 band spectra from the Jupiter nightside from January 20, 2001, are shown. Reflected sunlight is now negligible at the long wavelengths in the FUV. Torus sulfur emissions are seen near 170 nm. Also shown are UVIS lab spectra obtained pre-launch of 100 eV electron impact on H_2 gas. Jupiter's spectrum resembles the laboratory spectrum in the FUV, but not in the EUV due to H_2 self-absorption effects in the jovian atmosphere. Attenuating the lab spectrum by adding a simulated absorbing layer of CH_4 (column density of 3×10^{16} cm^{-2}) above the emission improves the overall shape agreement. Adding some C_2H_2 (column density of 1×10^{15} cm^{-2}) improves the fit near 152 nm, but worsens the fit near 130 nm.

complex mosaics, slews, and maps of the closest approach time period make that data more suitable for detailed spectroscopy studies presented elsewhere (Ajello et al., 2005) than global output studies.) Data were used from the UVIS EUV channel in the 110.8–113.1-nm region and the FUV channel from 127.1 to 128.9 nm for monitoring H_2 band emissions, since these wavelength regions included Jupiter emissions but were free of contamination from bright emissions seen in UVIS observations viewing the Io plasma torus (Steffl et al., 2004a, 2004b). Fig. 4 shows the observing geometry for one of these spatially unresolved auroral observations.

The UVIS time-series data in Figs. 5 and 7 revealed a surprising amount of structure that is not due to counting sta-

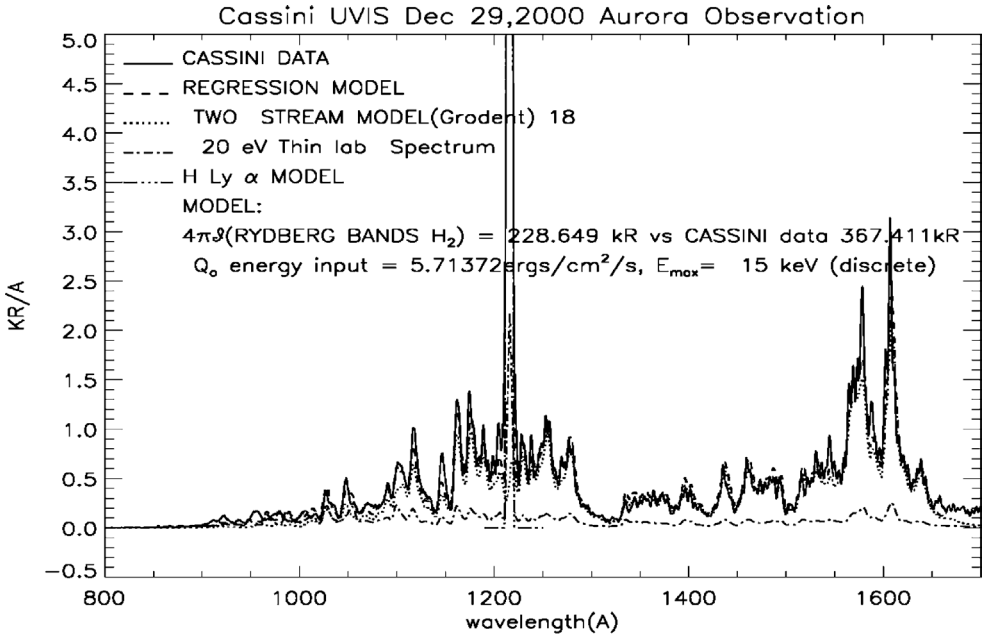

Fig. 3. Initial modeling efforts of the merged UVIS EUV/FUV spectrum from December 29, 2000. In this case 3 model components were compared to the data: a two-stream electron energy deposition model by Grodent, an optically thin 20 eV electron impact on H_2 spectrum, and a separate fit to the Lyman-α line shape based on interplanetary Lyman-α data. A multiple linear regression combination of these 3 components fits the data.

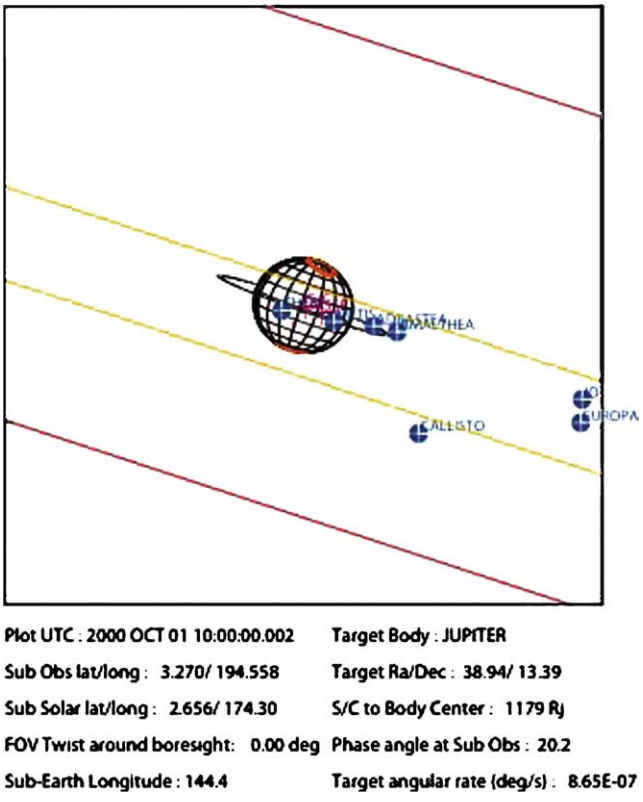

Fig. 4. Sample geometry from October 1, 2000, for the UVIS globally integrated auroral observations. In this case the long slits were aligned east–west on Jupiter at a range of 1179 Jupiter radii from Cassini and a phase angle of 20.2°. The wide slit (red) is the EUV, that observed the entire planet. The narrower slit (yellow) is the FUV. Reference auroral ovals are indicated in orange. The FUV only captured the southern auroral zone and part of the disk in the time-series data.

tistics. Large UV brightening events were seen, each lasting for several hours and covering a variety of Central Meridian Longitudes (CML). Exact event durations are unclear because of the data-taking sampling. Several-hour periods of UVIS data were separated by several-hour periods when CAPS full solar wind data was taken. Large-scale UV brightening events were seen in both the approach data (low phase angle, dayside), and in the outbound data at high phase angles that probably represent mostly nightside auroral activity. The 2 brightest events were on days 280 and 325–326 of 2000, when UV auroral emissions were enhanced by a factor of 2–4. The same structures in the auroral time-series data are seen in both the FUV and EUV channels in periods when both channels observed the auroral zones (Fig. 5). Fig. 6 shows the spectrum of the day 280 event, compared to spectra obtained under more normal conditions. The overall effect of this event is an auroral brightening, and not an obvious change in the spectral appearance, as might be expected from an increase in mean particle energy that would lead to increased hydrocarbon absorption at short wavelengths in the FUV channel. In other words, the brightening appears to be related to an increase in precipitating particle flux and not to an increased particle mean energy. To quantify this result, the day 280 FUV event spectrum can be fit (Fig. 6, middle panel) with the following expression:

$$\text{Cts (day 280)} = A \times \text{Cts (disk)} + B \times \text{Cts (lab)} \times \exp(\text{CH}_4 \text{ column density} \times \sigma_{\text{CH}_4}),$$

where Cts is the FUV counts spectrum, Cts (day 280) is the FUV day 280 event spectrum, Cts (disk) is an FUV counts spectrum from the period around day 320 when the FUV channel was viewing the disk and not the auroras,

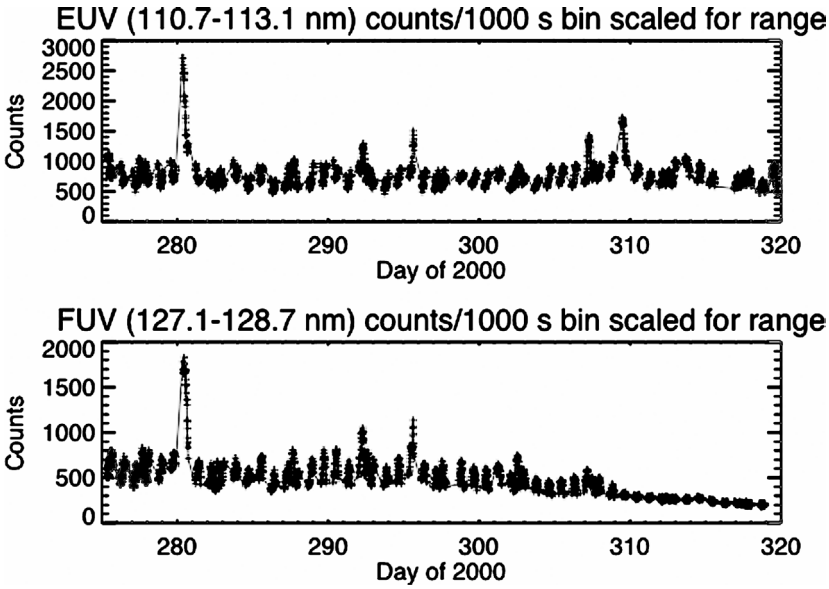

Fig. 5. The early approach auroral time-series from UVIS EUV (watching both poles) and FUV (watching the S pole and disk center early, and just disk center late in the period). The early data are correlated, showing that the outbursts occurred in the S and perhaps also in the N.

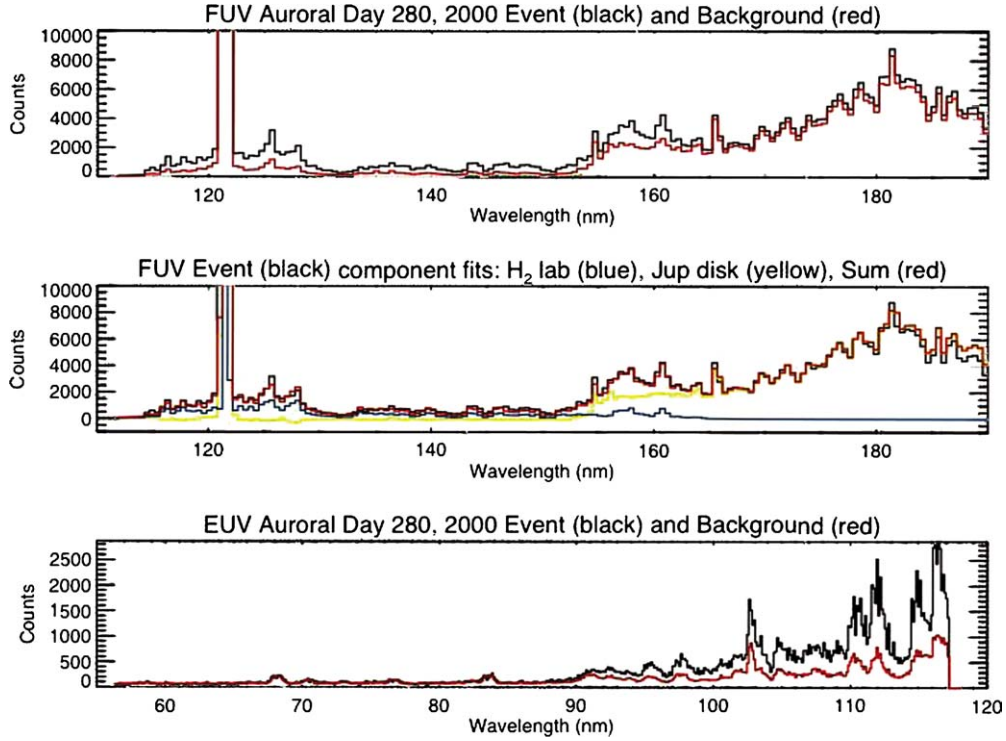

Fig. 6. The spectrum of the strong event on day 280 of 2000 (in counts/1000 s integration/bin) is compared to the average of 100,000 s of data from the previous week. Top panel: FUV data. Both spectra show reflected Jupiter signal at long wavelengths. Near and below 160 nm the H_2 band emissions dominate. The off-scale emission is Lyman-α at 121.6 nm. Middle panel: The FUV day 280 event spectrum can be matched by combining a non-auroral reflected sunlight spectrum from Jupiter and a lab spectrum of electron impact on H_2 attenuated by a methane column density of 3×10^{16} cm^{-2}. Bottom panel: EUV data. At short wavelengths Io plasma torus lines are seen such as SIII 68.5 nm and OII, OIII 83.4 nm emissions. Above about 85 nm H_2 bands emission from Jupiter's auroras are seen.

Cts (lab) is the pre-flight electron impact on H_2 lab spectrum, A and B are fitting parameters, σ_{CH_4} is the methane cross-section (cm^2), and the derived CH_4 column density for both the event and the preceding days is estimated to be $3 \pm 1 \times 10^{16}$ cm^{-2}. That is, the auroral event occurred at about the same mean methane column density in the atmosphere as the background auroral situation.

Fig. 7 shows the complete set of disk-integrated EUV observations of Jupiter, showing a number of enhanced emission events, including events on 2000 days 280, 307–309,

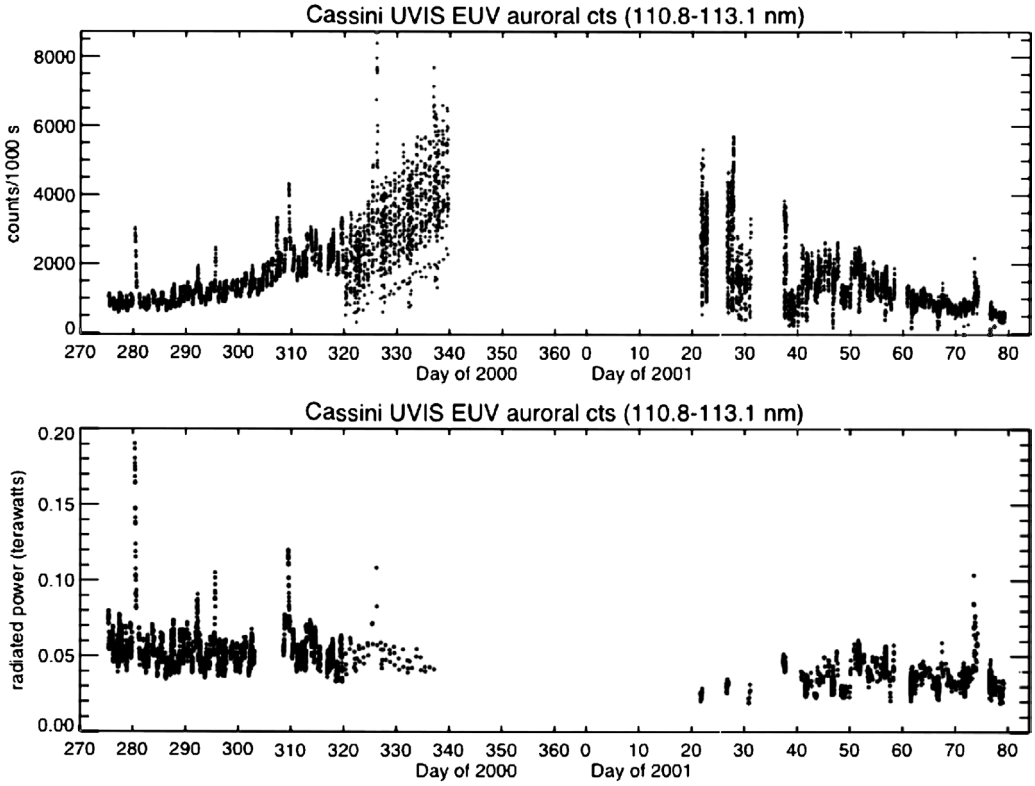

Fig. 7. Time-series of the EUV auroral emissions seen by Cassini UVIS during the encounter with Jupiter. Both poles were in the slit. Several statistically significant brightening events were seen. The top panel shows count-rates vs time. The bottom panel shows radiated power for those observations in which Jupiter was fully in the EUV observing slit.

325–326, and 2001 day 73. The top panel shows the count-rates vs time. The bottom panel shows the radiated power from Jupiter for selected observations in which Jupiter was fully in the slit. This filtered data set removes most of the lowest points, and also some of the highest ones during auroral storms. The filtered inbound data obtained near 20° phase angle are systematically higher than the filtered outbound data obtained near 140° phase angle. This could be due to auroral differences, but this is also the expected phase angle behavior for the dayglow component, which is not clearly separated from auroral emissions in these observations.

An improved way to look at the trend in the auroral data is to remove the modulation from the time-series due simply to Jupiter's rotation. This was accomplished using HST STIS auroral images (like the one in Fig. 8) that indicate the projected area of the main auroral ovals in the north and south that was in view at any given CML. A linear least-squares fit between auroral area visible and UV count rate of the form

$$\text{fit to UV count rate} = \text{constant} + \text{slope} \times \text{visible auroral area}$$

(Fig. 9) leads to an expected modulation curve, that can be subtracted from the count-rate curve to leave a residual curve that emphasizes the auroral storms (bottom panel, Fig. 14). This approach removes much of the variance.

4. Comparisons with other data sets

Radio observations of Jupiter show some of the same brightening events that UVIS observed. Comparisons at hectometric wavelengths of the UVIS data and the hectometric Cassini RPWS data are shown in Fig. 10 for the 2000 day 280 auroral event. The radio data have the advantage of being continuous. The UVIS data and the RPWS data have similar increases in brightness. Fig. 11 compares weaker brightening events from 2000 days 307–309 for the 2 instruments, again showing increases in both.

A variety of observations allow us to examine the 2000 days 325–326 Jupiter auroral brightening event in some detail. The event is linked to a strong solar flare and coronal mass ejection (CME) on 2000 day 313 (November 8). Because Jupiter opposition occurred on day 331 (November 26), Jupiter and Earth were almost radially aligned with the Sun on November 8, so solar wind observations obtained near Earth are relevant to the events on Jupiter. The CME was observed by the Solar Heliospheric Observatory (SOHO) LASCO (Large-Angle and Spectrometric Coronagraph Experiment) C3 instrument. The CME reached Earth on day 315, when SOHO, ACE (Advanced Composition Explorer) and other spacecraft observed a strong shock in the solar wind, characterized by a jump in velocity, density, and temperature (http://www.spaceweather.com). This was the largest of several large CMEs that merged to form a larger

Fig. 8. HST STIS UV image of Jupiter's north polar auroral H_2 Werner and Lyman band and H Lyman-α emissions from November 26, 1998. The almost complete oval is the main oval. The arc-like feature at lower latitudes near the left limb is related to the Io–Jupiter current system. Emissions inside the main oval are highly variable.

merged interaction region before reaching Jupiter (Hanlon et al., 2004). The merged CME shock reached Cassini (which was upstream of Jupiter) on day 323 at 17 h and reached Galileo (closer to Jupiter) on day 324 at 9 h. Enhanced solar wind density measured by Cassini CAPS, magnetic field magnitude measured by Cassini MAG, and energetic ion and electron density measured by Galileo EPD persisted for several days, overlapping with the days 325–326 auroral event (Figs. 12–14).

The more complete Cassini RPWS (radio) time-series data show several periods of enhanced hectometric radio emission during the passage of large coronal mass ejection events (Gurnett et al., 2002). One of these is associated with the days 325–326 auroral event seen in UVIS. Other radio flux increases occurred when UVIS was not taking data. The flux increases in the radio, like the UV, were increases of up to a factor of 3–4. In general, the hectometric radio emissions vary out of phase of the auroral emissions (Fig. 9). This is due to the preferential emission of the radio beam in a hollow cone at a particular angle to the local magnetic field produced by spiraling electrons. For example, 1–10-keV auroral electrons emit radio waves at ∼80° to the local magnetic field direction, in a cone ∼10° wide (Ladreiter and Leblanc, 1989; Ladreiter, 1991).

ACE data for this large CME event at Earth were used to simulate the effect on Jupiter's magnetosphere of the CME. This was done using a 1-D MHD simulation developed at the University of Michigan to propagate the solar wind radially from Earth to Jupiter. The MHD simulation supplements the spotty solar wind coverage available at Cassini (because of spacecraft constraints, when full solar wind data was obtained, auroral data was not, so time-sharing took place). Fig. 14 illustrates this comparison. Agreement is not complete, reflecting the limitations of 1-D models, although it does generally indicate the several-day period of enhanced solar wind density and enhanced auroral activity. A similar MHD calculation has indicated that the same shock responsible for the 2000 days 325–326 auroral event at Jupiter may also be responsible for an auroral storm at Saturn detected in HST observations (Prange et al., 2004).

5. UVIS high-time-resolution auroral data

On January 8, 13, and 20–21, 2001, Cassini UVIS obtained data in a special high time-resolution mode. These observations were part of a campaign with simultaneous HST STIS observations. Fig. 15 shows the locations of the Cassini spacecraft during these campaign observations. Instead of the typically 1000-s UVIS integrations described earlier, 4-s integrations were obtained to look for rapid auroral variations. This high time-resolution data was obtained with reduced spectral and spatial resolution, with just 16 spectral and 16 spatial bins for each of the EUV and FUV channels. Fig. 16 shows a sample observing geometry for January 8, 2001. The long slit spectrometer was aligned N–S, allowing for spectral separation of the 2 polar regions. Fig. 17 shows a spectrum obtained in this mode, showing H_2 band emission in both the EUV and FUV, and Lyman-α emission in the FUV. At the longest wavelengths in the FUV, sunlight that has been Rayleigh-scattered by Jupiter's hydrogen and helium gas is visible. Fig. 18 shows time-series data obtained on January 8, 2001 for both the FUV and EUV data for the north polar region. Fig. 18 (and Figs. 19, 20, 22, and 23) shows selected EUV wavelengths from 95.0 to 114.3 nm and FUV wavelengths from 136.4 to 166.3 nm, avoiding most of the Lyman-α emission that includes a substantial component of dayglow as well as auroral emissions. The period from January 8 18:45–19:35 h appeared particularly interesting, showing a series of almost periodic bursts of UV radiation that persist for typically a minute or two with separations of a few minutes. These periodic bursts are subtle features in the intensity, representing only ∼20% enhancements, unlike the major storms described earlier that increased the UV output by factors of 3 or 4. The periodic bursts spectral signature (color ratio, etc.) is difficult to determine from this limited spectral resolution data set because Lyman-α from dayglow and aurora is blended with short-wavelength H_2 band emission. At 19.0 h the Cassini subspacecraft longitude was 173°, an almost ideal position for viewing the magnetic north pole, which is substantially offset from the rotation axis. Fig. 19 shows just this selected time period, showing that the EUV and FUV variations occur together. Fig. 20 il-

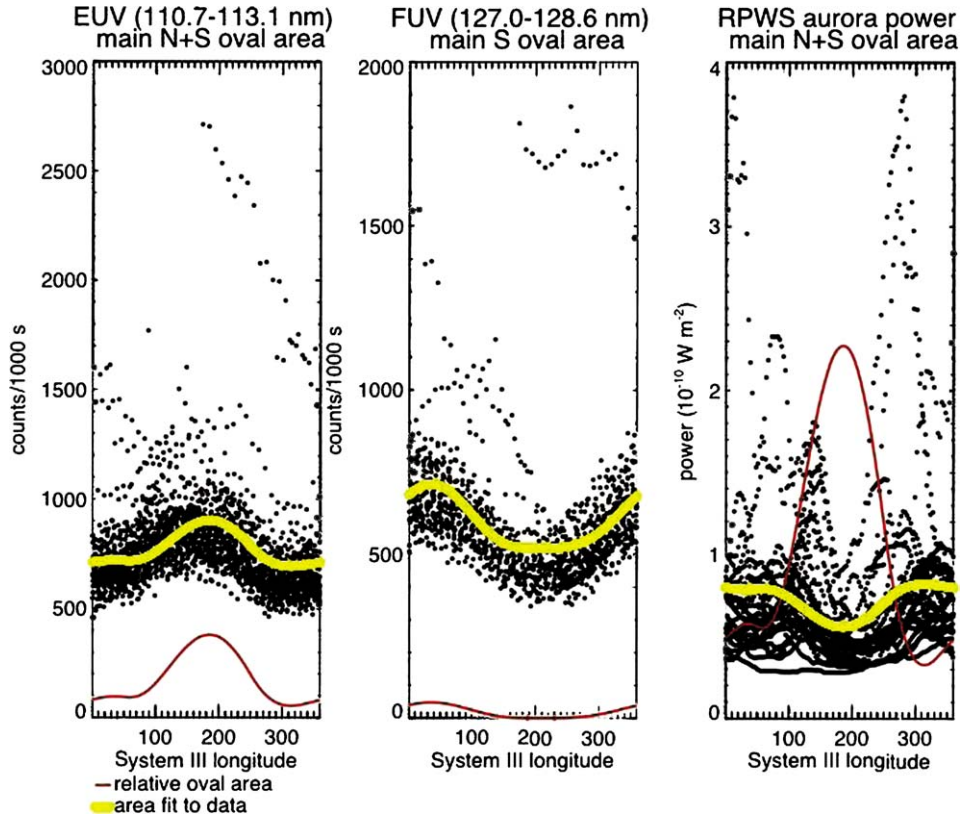

Fig. 9. Left panel: The time-series EUV auroral data (range-corrected counts per integration period) from both poles from 2000 days 275–339 are well correlated with the relative main auroral arc area from both north and south visible at any central meridian longitude (red line). The arc area at each longitude was determined from HST STIS imaging data. The yellow line is the least squares fit of the auroral area to the data. Auroral outbursts are seen to be present as high data points seen at a variety of longitudes. Middle panel: The time-series FUV auroral data from the south pole from 2000 days 276–302 are well correlated with the relative main south auroral arc area visible at any central meridian longitude (red line). The yellow line is the least squares fit of the auroral area to the data. Southern auroral outbursts are seen to be present as high data points seen at a variety of longitudes. Right panel: Cassini RPWS relative intensity on 2000 days 322–332, unlike the UVIS data in the first two panels, is out of phase with the relative total auroral area (red) visible at any central meridian longitude. A fit of the relative area to the data (yellow) shows how out of phase the UV and radio emissions are. Although the major auroral outbursts are seen in both the radio and the UV, detailed agreement should not be expected due to radio beaming effects.

lustrates the linear relationship between the EUV and FUV emissions in this period.

The UV variations in UVIS data on short timescales seem similar to bursty emissions in the interior of the auroral main ovals seen in earlier HST STIS UV data (Waite et al., 2001; Pallier and Prange 2001, 2004; Gerard et al., 2003), Galileo UV data (Pryor et al., 2001) and Chandra X-ray data (Gladstone et al., 2002). The ∼2-min duration and quasi-periodic nature of the UV variations found here reminded us of earlier work on quasiperiodic (QP) radio bursts at Jupiter (Kurth et al., 1989; MacDowall et al., 1993; Desch, 1994; Kaiser et al., 2001; Hospodarsky et al., 1998, 2001, 2003, 2004). We examined Cassini Radio and Plasma Wave Subsystem (RPWS) (Gurnett et al., 2002) 6–10 kHz data for the January 8, 2001 18.6–19.7-h period and found little correlation with the Cassini UV data. However, the Galileo Plasma Wave Subsystem (Gurnett et al., 1992) was at a similar jovian longitude in this period (at 19:00 h Galileo was at 213° subspacecraft longitude vs 174° for Cassini, and closer to the planet, 91 Jupiter radii vs 185, and at a smaller local time, 16.3 vs 19.0 h for Cassini), and we compared 0.6–5-kHz data from Galileo PWS (Fig. 21) to the UVIS variations seen in the northern auroral zone from 18.75 to 19.6 h (Fig. 22). In this case the linear correlation between the variations in the 2 instruments is good (Figs. 22 and 23) with a linear correlation coefficient $r = 0.57$ with the chance of the correlation being random (P) of less than 0.001 (Bevington, 1969). Detailed agreement between UV and quasiperiodic radio emissions may be possible because these low frequency radio emissions are not strongly beamed and can be seen from a wide range of angles (Hospodarsky et al., 2004). The reason that the Galileo radio data are well correlated with UVIS data, while the Cassini radio data are not, is probably because the radio emissions were already difficult to detect at Galileo, and were below the detection threshold at Cassini, which was further from Jupiter.

Supporting HST observations, although planned, were not obtained on January 8, 2001 when the UVIS quasiperiodic bursts were seen. However, HST STIS observations were obtained on January 13 and January 20–21 when UVIS was observing. Unfortunately, the UV variations seen in

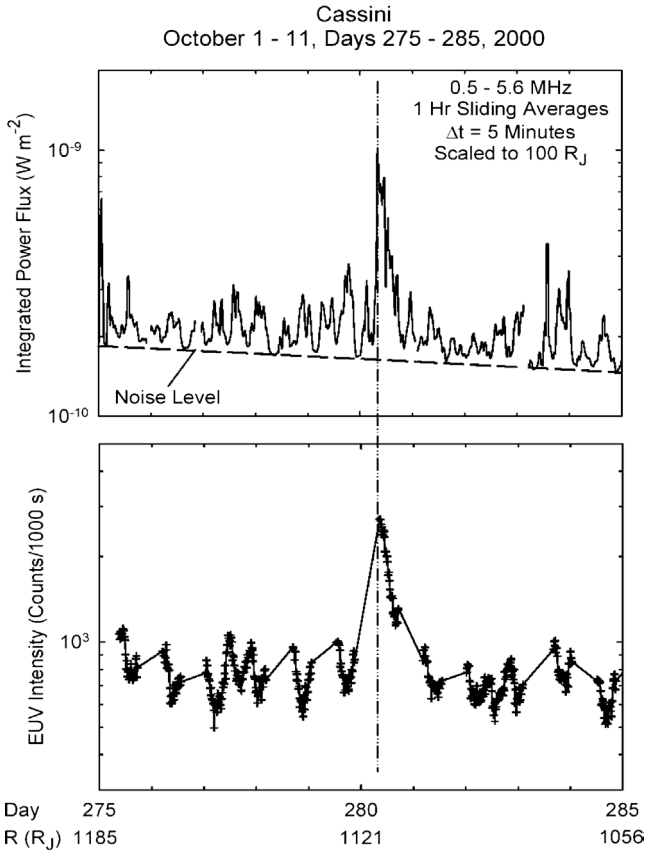

Fig. 10. The first large auroral outburst seen in the UVIS EUV auroral time-series data on 2000 day 280, also occurred in the more continuous Cassini RPWS hectometric data, with similar increases in relative intensity. The UVIS data points are indicated by + symbols, with the line between + signs just there to guide the eye. The radio outburst begins more abruptly than it ends.

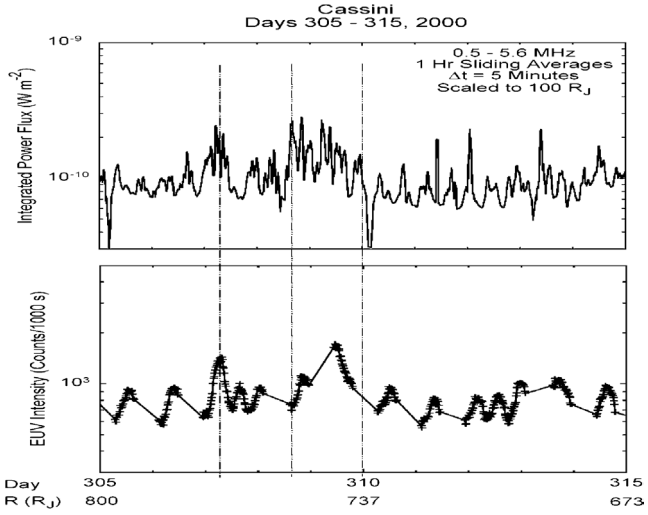

Fig. 11. Enhanced auroral activity seen in the UVIS EUV auroral time-series approach data on 2000 days 307–309, also occurred in the more continuous Cassini RPWS hectometric data, with similar increases in relative intensity. The UVIS data points are indicated by + symbols, with the line between + signs just there to guide the eye.

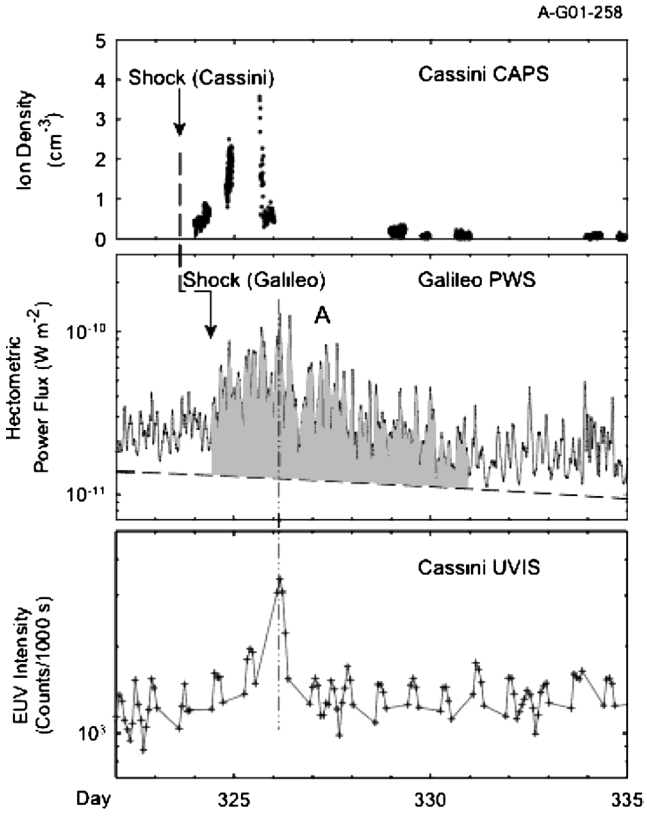

Fig. 12. The large auroral outburst seen in the UVIS EUV auroral time-series approach data on 2000 days 325–326, also occurred in the more continuous Cassini RPWS hectometric data, with similar increases in relative intensity. The UVIS data points are indicated by + symbols, with the line between + signs just there to guide the eye. The time of shock passage at Cassini on day 323 17 h is indicated. Cassini CAPS found enhanced ion densities after shock passage. Reprinted with permission from Gurnett et al. (2002).

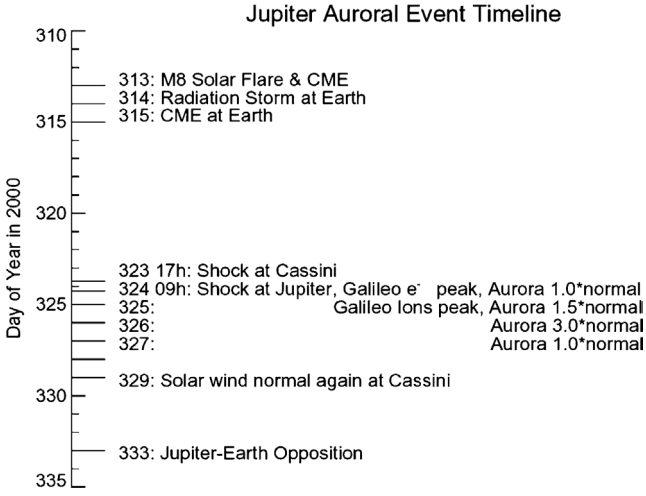

Fig. 13. Key events related to the days 325–326 Jupiter auroral events are indicated.

UVIS were much smaller on those days than on January 8. We did examine HST STIS time-tagged images from January 13, 2001 that show modest south polar auroral zone flares in the interior of the main oval. During this period lit-

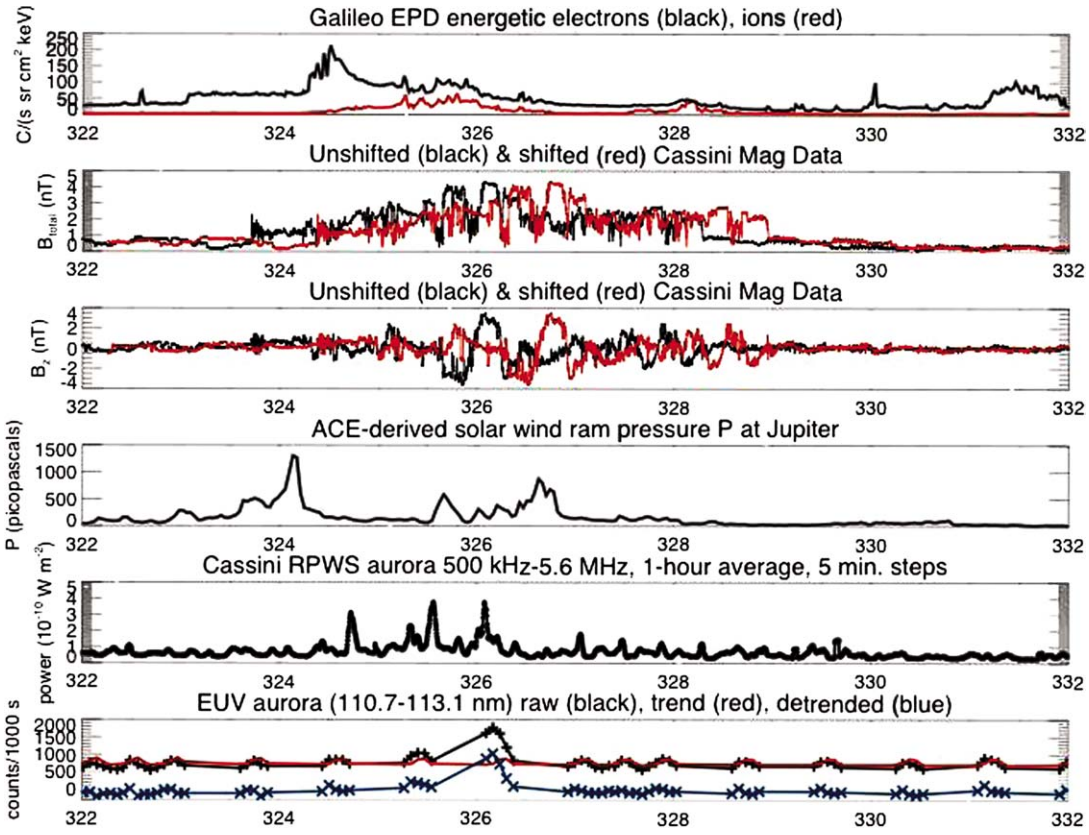

Fig. 14. The auroral event from days 325–326 was related to passage of a CME that affected several experiments. Top panel: Galileo EPD data indicate a sharp increase in energetic electrons and ions on day 324 that persisted for several days. 2nd and 3rd panels: Cassini total magnetic field and z-component magnetic field data indicate enhanced magnetic fields and several z-component reversals from day 323 to day 328. The data are also displayed with a 16-h delay to line up the shock seen at Cassini with the shock detected on day 324 by Galileo EPD. 4th panel: Estimated solar wind ram pressure based on ACE data at 1 AU propagated to Jupiter by an MHD code. 5th panel: Cassini RPWS data show several radio bursts associated with the CME passage. 6th panel: UVIS EUV data (black) show the major event seen in the radio data on day 326. The red curve shows the expected variations based solely on rotation of a static oval. Also shown is the UVIS data detrended (blue): the red curve has been subtracted from the black.

tle variation was evident in the less spatially resolved UVIS data. The STIS data sets support the idea that most auroral variations on short timescales occur in the interior of the main auroral oval, something that the UVIS data do not have the spatial resolution to show unambiguously. Additional discussion of the HST STIS data for the campaign period can be found in Grodent et al. (2003).

6. Conclusions

UVIS has created a rich database of Jupiter auroral spectra that show the presence of well-defined auroral brightenings, or storms. These UVIS brightenings occur together with hectometric radio brightenings measured by Galileo PWS and Cassini RPWS that include more complete time-coverage. These combined observations demonstrate that Jupiter's aurora responded strongly to the compression events produced when large solar coronal mass ejections reached Jupiter's magnetosphere. Earlier work with Ulysses, Galileo and IUE data also indicated that CME's can drive auroral brightenings (Prange et al., 1993, 2001). We conclude that, at least occasionally, the solar wind plays a major role in the Jupiter system, in spite of the rich plasma source at Io, and the vast rotational energy in the system. More generally, Jupiter's main auroral emissions are thought to be associated with co-rotation breakdown in the middle part of the Io-plasma dominated magnetosphere (e.g., Cowley et al., 2003). This is a different situation from the Earth, where the main auroral emissions are associated more directly with the polar cap boundary layer and solar wind effects (e.g., Tsurutani et al., 2002).

It is not yet clear from these globally integrated UVIS observations what type of aurora the several-day-long auroral storms represent. The auroral storms reported here may occur on the main oval, where most of the emissions occur, due to compression of the whole magnetosphere by increased solar wind ram pressure, or perhaps in the polar cap, where highly variable auroras have been seen (e.g., Waite et al., 2001; Pryor et al., 2001; Gladstone et al., 2002; Grodent et al., 2003). We do know from the UVIS outbursts seen at both low phase angles on approach and high phase angles on the dusk side during the outbound phase that UVIS was not just seeing the dawn storms, bright spots near dawn

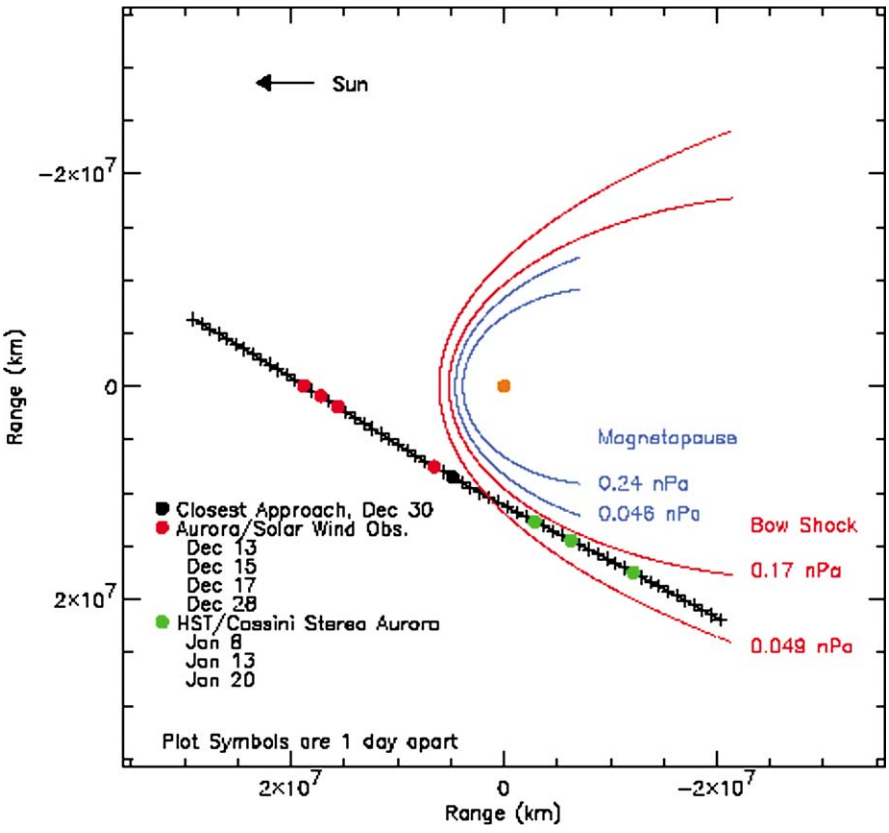

Fig. 15. The Cassini/HST observing campaign. The Cassini trajectory, with 1-day time ticks, is shown near representations of the jovian bow shock and magnetopause for two different solar wind pressure values. UVIS time-resolved observations occurred where the 3 green dots occur, on the dusk side, slightly towards midnight local time. HST observations occurred when Cassini was at the locations of the 4 red dots and the last 2 green dots. The HST observations did not occur on January 8, 2001.

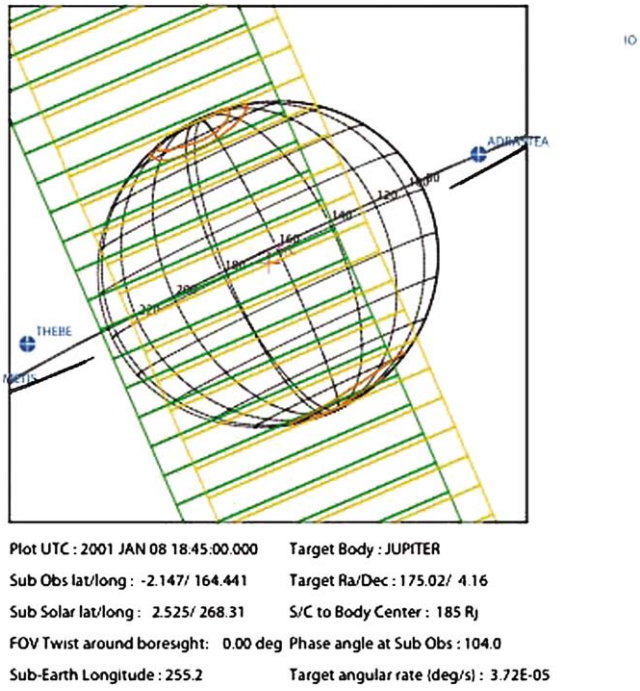

Fig. 16. Observing geometry for the January 8, 2001, observations at 18:45. The UVIS long slits (EUV green, FUV yellow) are aligned N–S, providing 64 spatial bins. 16 bins were returned in the data stream. At this time the northern auroral oval was clearly in view.

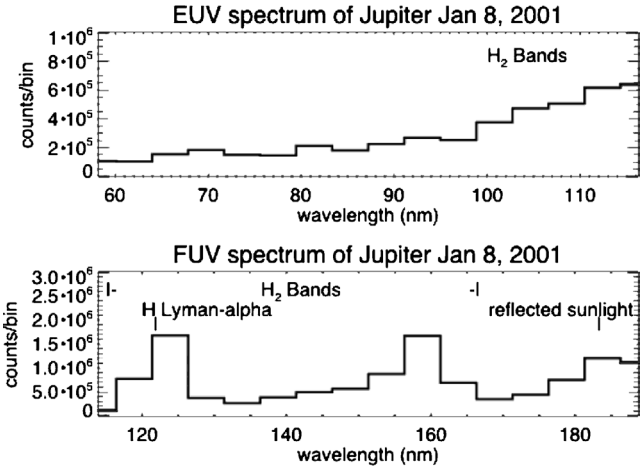

Fig. 17. High-time resolution spectra from January 8, 2001, have been summed to show the H_2 band emission in both channels and the H Lyman-α 121.6-nm emission in the FUV channel.

sometimes seen on the main auroral ovals (e.g., Ballester et al., 1996).

Recent theoretical work had suggested (Southwood and Kivelson, 2001, and Cowley et al., 2003) that the most important effect on Jupiter's aurora would be a dimming during magnetospheric compression and a brightening when the

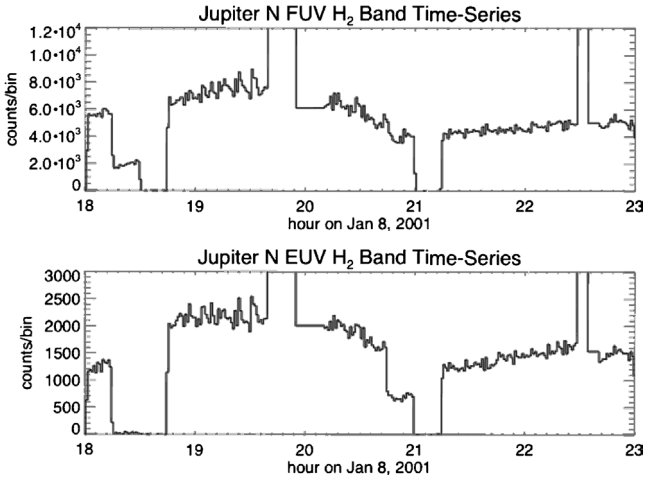

Fig. 18. 5 h of Cassini UVIS high time resolution data are presented from January 8, 2001, with the FUV in the top panel and the EUV in the bottom panel. Notice the large, statistically significant, almost periodic variations from 18:45–19:35 (18.75–19.6) h. Sudden large rises and falls indicate spacecraft slews.

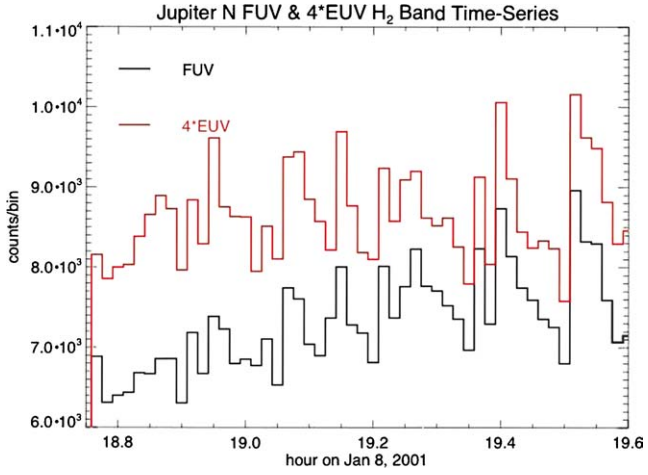

Fig. 19. The counts/bin variations in the Cassini UVIS EUV and FUV channels are seen to track each other in the period from 18.75 to 19.6 h on January 8, 2001.

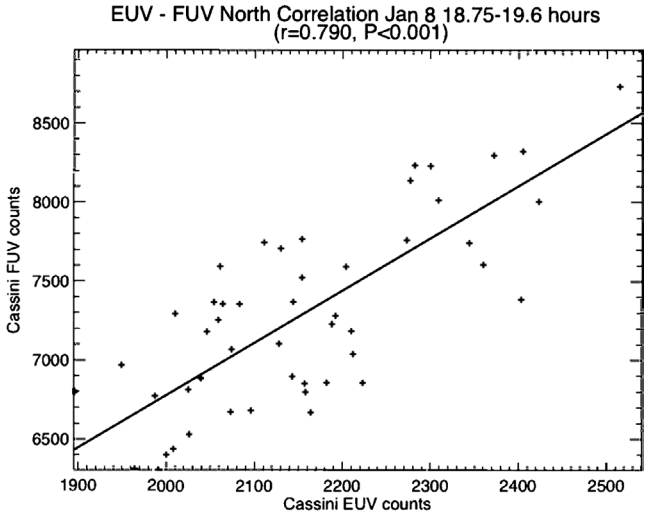

Fig. 20. Linear regression showing that the UVIS EUV and FUV high-time resolution auroral variations from Fig. 19 are linearly correlated.

compression ended, the opposite of what is described here. For the Earth, it has been shown that CME pressure pulses can drive auroral brightenings (Zhou and Tsurutani, 1999, 2001). The effects of CMEs on the Jupiter magnetosphere are clearly not well understood. Better data are needed from future missions to resolve these issues.

The quasiperiodic UV data presented here indicate that there is a connection between quasiperiodic low-frequency radio bursts (0.6–5 kHz) and UV flares of ∼1–2-min duration in the interior of the main auroral oval that have been seen in both polar regions. In the Cassini at Jupiter era, quasiperiodic radio bursts exhibit a wide variety of durations and separations, with a common separation interval between bursts of 1–2 min (Kaiser et al., 2001). Initial direction finding efforts with Cassini and Galileo radio data found a high-latitude source for quasiperiodic bursts near the magnetopause (Hospodarsky et al., 2004) perhaps in reconnection events. Energetic particle bursts seen in Ulysses data may also be related to quasiperiodic radio bursts (Zhang et al., 1993; McKibben et al., 1993). There is a terrestrial analog to the QP bursts called low-frequency (LF) bursts that are primarily correlated with solar wind velocity, with some dependence on interplanetary magnetic field orientation (Desch et al., 1996; Kaiser et al., 2001).

These bursty events may be the source of the jovian relativistic electrons that have been observed near Earth in recent years by the SAMPEX spacecraft (Kanekal et al., 2003). In Pioneer 11 data from 1974 these jovian relativistic electrons were enhanced during periods of reduced solar wind dynamic pressure (Morioka and Tsuchiya, 1996). During the Cassini epoch mono-directional energetic electron bursts were detected escaping from the dusk magnetosphere (Krupp et al., 2002, 2004) when Cassini was outside the magnetopause. On January 10, 2001, when both Cassini and Galileo were inside the magnetopause, bi-directional electron beams were observed: Cassini observed 40-min periodic electron modulation, while Galileo observed 60-min periodic modulations. It is not yet clear what causes the multiple periodicities in what may be a bursty reconnection process. Systematic study of bursty events in Galileo EPD data led Woch et al. (2002) to deduce the presence of a near Jupiter neutral line where reconnection is taking place, and which they identify with the origin of both the auroral flares (inside the main oval) and the auroral dawn storms that fall on the main auroral oval. Bunce et al. (2004) recently presented a theoretical model for producing the polar cap "cusp" auroras from pulsed reconnection at the dayside magnetopause.

It will be valuable to pursue auroral flare and radio burst comparisons using ground-based infrared H_3^+, CH_4, C_2H_2, and C_2H_6 band emission data and HST UV and Chandra

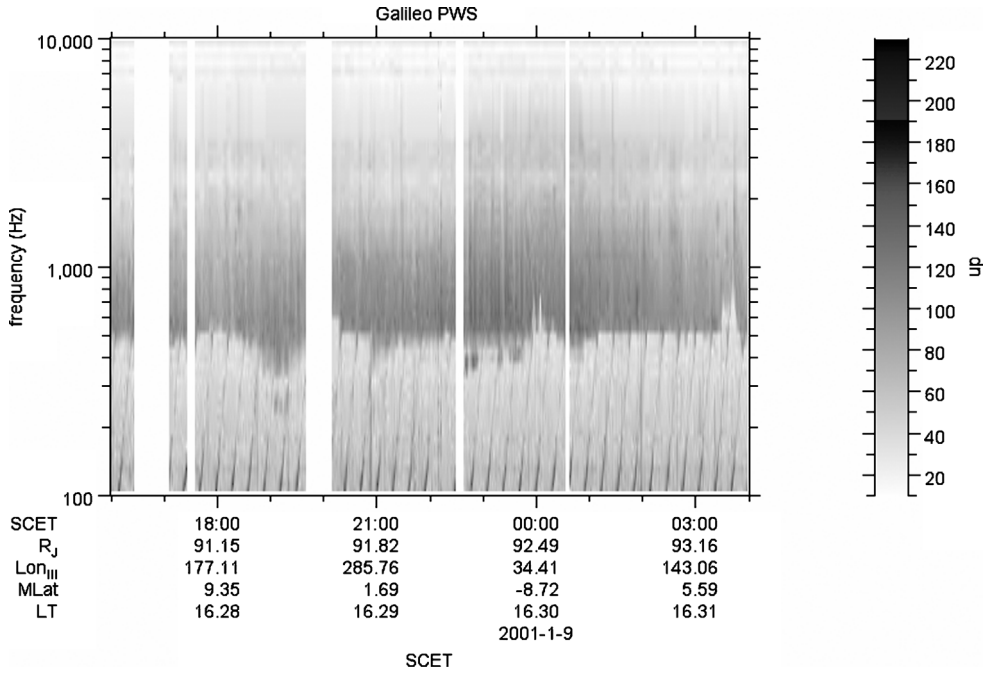

Fig. 21. Galileo PWS spectrogram showing the power level as a function of time and frequency including the period under study from 2001 day 8 18.75 to 19.6 h.

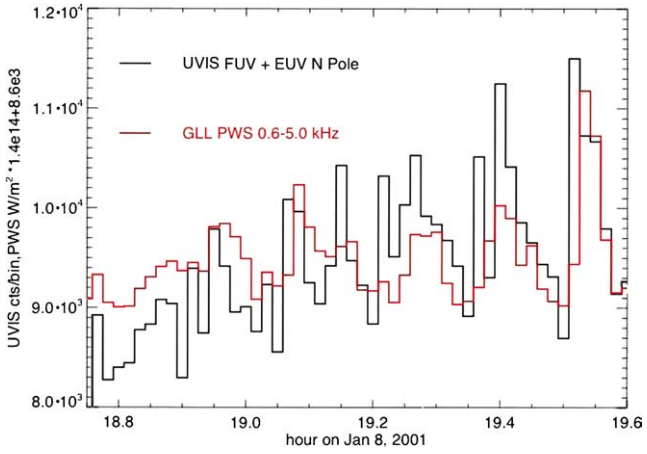

Fig. 22. The sum of the EUV and FUV H_2 band counts from the northern auroral zone are compared with the Galileo PWS radio signal from 0.6 to 5.0 kHz for the period 2001 day 8 18.75–19.6 h.

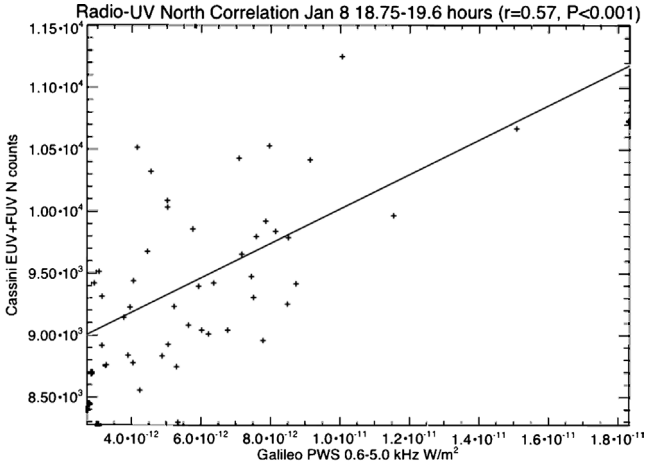

Fig. 23. Linear regression showing that the sum of the UVIS EUV and FUV H_2 band counts from Jupiter's northern auroral zone is linearly correlated with the Galileo PWS radio signal from 0.6 to 5.0 kHz for the period 2001 day 8 18.75–19.6 h.

X-ray observations of the Jupiter auroral emissions obtained while Ulysses made its second Jupiter encounter with a closest approach on February 4, 2004, of 1684 Jupiter radii. Ulysses has been observing quasiperiodic Jupiter radio bursts (MacDowall et al., personal communication, 2002) with the URAP (Ulysses Radio Astronomy Package, Stone et al., 1992).

The Cassini UVIS data from Jupiter encounter contain a great deal of information about auroral processes. Another UVIS study details the auroral spectroscopy from closest approach (Ajello et al., 2005). We look forward to many Cassini auroral observations of Saturn in the coming years.

Acknowledgments

We acknowledge support for this work from the Cassini and Galileo Projects and from the Space Telescope Science Institute. W. Pryor acknowledges support from the University of Colorado, Central Arizona College, the NASA Office of Space Science Minority University Initiative at Hampton University, the NASA Planetary Atmospheres Program and the NASA Jupiter System Data Analysis Program. Portions of this work were performed at the Jet Propulsion Laboratory, California Institute of Technology under contract with NASA. Portions of this work are based on observations

with the NASA/ESA Hubble Space Telescope, obtained at the Space Telescope Science Institute, which is operated by AURA, Inc., for NASA.

References

Ajello, J., Shemansky, D., Pryor, W., Tobiska, K., Hord, C., Stephens, S., Stewart, I., Clarke, J., Simmons, K., McClintock, W., Barth, C., Gebben, J., Miller, D., Sandel, B., 1998. Galileo orbiter ultraviolet observations of Jupiter aurora. J. Geophys. Res. 103, 20125–20148.

Ajello, J.M., Shemansky, D.E., Pryor, W.R., Stewart, A.I., Simmons, K.E., Majeed, T., Waite, J.H., Gladstone, G.R., Grodent, D., 2001. Spectroscopic evidence for high-altitude aurora at Jupiter from Galileo Extreme Ultraviolet Spectrometer and Hopkins Ultraviolet Telescope observations. Icarus 152, 151–171.

Ajello, J.M., Pryor, W.R., Esposito, L.W., Stewart, A.I.F., McClintock, W.E., Gustin, J., Grodent, D., Gerard, J.-C., Clarke, J.T., 2005. The Cassini Campaign observations of the Jupiter aurora by the Ultraviolet Imaging Spectrograph and the Space Telescope Imaging Spectrograph. Icarus 78, 327–345.

Ballester, G.E., Clarke, J.T., Trauger, J.T., Harris, W.M., Stapelfeldt, K.R., Crisp, D., Evans, R.W., Burgh, E.B., Burrows, C.J., Casertano, S., Gallagher III, J.S., Griffiths, R.E., Hester, J.J., Hoessel, J.G., Holtzman, J.A., Krist, J.E., Meadows, V., Mould, J.R., Sahai, R., Scowen, P.A., Watson, A.M., Westphal, J.A., 1996. Time-resolved observations of Jupiter's far-ultraviolet aurora. Science 274, 409–412.

Bevington, P.R., 1969. Data Reduction and Error Analysis for the Physical Sciences. McGraw–Hill, New York.

Bhardwaj, A., Gladstone, G.R., 2000. Auroral emissions of the giant planets. Space Sci. Rev. 38, 295–353.

Bolton, S.J., Janssen, M., Thorne, R., Levin, S., Klein, M., Gulkis, S., Bastian, T., Sault, R., Elachi, C., Hofstadter, M., Bunker, A., Dulk, G., Gudim, E., Hamilton, G., Johnson, W.T.K., Leblanc, Y., Liepack, O., McLeod, R., Roller, J., Roth, L., West, R., 2002. Ultra-relativistic electrons in Jupiter's radiation belts. Nature 415, 987–991.

Bunce, E.J., Cowley, S.W.H., Yeoman, T.K., 2004. Jovian cusp processes: Implications for the polar aurora. J. Geophys. Res. 109, doi:10.1029/2003JA010280.

Clarke, J.T., Ajello, J., Ballester, G., Ben Jaffel, L., Connerney, J., Gerard, J.-C., Gladstone, G.R., Grodent, D., Pryor, W., Trauger, J., Waite Jr., J.H., 2002. Ultraviolet auroral emissions from the magnetic footprints of Io, Ganymede, and Europa on Jupiter. Nature 415, 997–1000.

Cowley, S.W.H., Bunce, E.J., Nichols, J.D., 2003. Origin of Jupiter's main oval auroral emissions. J. Geophys. Res. 108, doi:10.1029/2002JA009329.

Desch, M.D., 1994. Jupiter radio bursts and particle acceleration. Astrophys. J. Suppl. Ser. 90, 541–546.

Desch, M.D., Kaiser, M.L., Farrell, W.M., 1996. Control of terrestrial LF bursts by solar wind speed. Geophys Res. Lett. 23, 1251–1254.

Dougherty, M.K., Kellock, S., Southwood, D.J., Balogh, A., Smith, E.J., Tsurutani, B.T., Gerlach, B., Glassmeier, K.-H., Gleim, F., Russell, C.T., Erdos, G., Neubauner, F.M., Cowley, S.W.H., 2004. The Cassini magnetic field investigation. Space Sci. Rev. 114, 331–383.

Esposito, L.W., Barth, C.A., Colwell, J.E., Lawrence, G.M., McClintock, W.E., Stewart, A.I.F., Keller, H.U., Korth, A., Lauche, H., Festou, M.C., Lane, A.L., Hansen, C.J., Maki, J.N., West, R.A., Jahn, H., Reulke, R., Warlich, K., Shemansky, D.E., Yung, Y.L., 2004. The Cassini ultraviolet imaging spectrograph investigation. Space Sci. Rev. 115, 294–361.

Gerard, J.-C., Gustin, J., Grodent, D., Clarke, J.T., Grard, A., 2003. Spectral observations of transient features in the FUV jovian polar aurora. J. Geophys. Res. 108, doi:10.1029/2003JA009901.

Gladstone, G.R., Waite, J.H., Grodent, D., Lewis, W.S., Crary, F.J., Elsner, R.F., Weisskopf, M.C., Majeed, T., Jahn, J.-M., Bhardwaj, A., Clarke, J.T., Young, D.T., Dougherty, M.K., Espinosa, S.A., Cravens, T.E., 2002. A pulsating auroral X-ray hot spot on Jupiter. Nature 415, 1000–1003.

Grodent, D., Waite Jr., J.H., Gerard, J.-C., 2001. A self-consistent model of the jovian auroral thermal structure. J. Geophys. Res. 106, 12933–12952.

Grodent, D., Clarke, J.T., Waite, J.H., Kim, J., Cowley, S.W.H., 2003. Jupiter's main auroral oval observed with HST–STIS. J. Geophys. Res. 108, doi:10.1029/2003JA009921.

Gurnett, D.A., Kurth, W.S., Shaw, R.R., Roux, A., Gendrin, R., Kennel, C.F., Scarf, F.L., Shawhan, S.D., 1992. The Galileo plasma wave investigation. Space Sci. Rev. 60, 341–355.

Gurnett, D.A., Kurth, W.S., Hospodarsky, G.B., Persoon, A.M., Zarka, P., Lecacheux, A., Bolton, S.J., Desch, M.D., Farrell, W.M., Kaiser, M.L., Ladreiter, H.-P., Rucker, H.O., Galopeau, P., Louarn, P., Young, D.T., Pryor, W.R., Dougherty, M., 2002. Solar wind control of jovian hectometric radio emission and auroral EUV emissions. Nature 415, 985–987.

Gurnett, D.A., Kurth, W.S., Kirchner, D.L., Hospodarsky, G.B., Averkamp, T.F., Zarka, P., Lecacheux, A., Manning, R., Roux, A., Canu, P., Cornilleau-Werlin, N., Galopeau, P., Meyer, A., Bostrom, R., Gustafsson, G., Wahlund, J.-E., Ahlen, L., Rucker, H.O., Ladreiter, H.P., Macher, W., Woolliscroft, L.J.C., Alleyne, H., Kaiser, M.L., Desch, M.D., Farrell, W.M., Harvey, C.C., Louarn, P., Kellogg, P.J., Goetz, K., Pederson, A., 2004. The Cassini radio and plasma wave investigation. Space Sci. Rev. 114, 395–463.

Gustin, J., Grodent, D., Gerard, J.C., Clarke, J.T., 2002. Spatially resolved far ultraviolet spectroscopy of the jovian aurora. Icarus 157, 91–103.

Gustin, J., Feldman, P.D., Gerard, J.-C., Grodent, D., Vidal-Madjar, A., Ben Jaffel, L., Desert, J.-M., Moos, H.W., Sahnow, D.J., Weaver, H.A., Wolven, B.C., Ajello, J.M., Waite, J.H., Roueff, E., Abgrall, H., 2004. Jovian auroral spectroscopy with FUSE: Analysis of self-absorption and implications for auroral precipitation. Icarus 171, 336–355.

Hanlon, P.G., Dougherty, M.K., Forsyth, R.J., Owens, M.J., Hansen, K.C., Toth, G., Crary, F.J., Young, D.T., 2004. On the evolution of the solar wind between 1 and 5 AU at the time of the Cassini Jupiter flyby: Multispacecraft observations of interplanetary coronal mass ejections including the formation of a merged interaction region. J. Geophys. Res. 109, doi:10.1029/2003JA010112.

Hill, T., 2002. Magnetic moments at Jupiter. Nature 415, 965–966.

Hospodarsky, G.B., Kurth, W.S., Gurnett, D.A., 1998. Galileo observations of jovian quasiperiodic radio bursts. Presented at the American Geophysical Union Meeting, Boston, MA.

Hospodarsky, G.B., Kurth, W.S., Gurnett, D.A., Kaiser, M.L., Zarka, P., Krupp, N., Waite, J.H., 2001. Quasiperiodic radio bursts as observed by Cassini and Galileo. Presented at the Fall AGU Meeting.

Hospodarsky, G.B., Kurth, W.S., Gurnett, D.A., Kaiser, M.L., Zarka, P., 2003. Simultaneous Observations of jovian quasiperiodic radio emission by the Cassini and Galileo spacecraft. Presented at the Fall AGU Meeting.

Hospodarsky, G.B., Kurth, W.S., Cecconi, B., Gurnett, D.A., Kaiser, M.L., Desch, M.D., Zarka, P., 2004. Simultaneous observations of jovian quasiperiodic radio emission by the Cassini and Galileo spacecraft. J. Geophys. Res. 109, doi:10.1029/2003JA010263.

Kaiser, M.L., Farrell, W.M., Desch, M.D., Hospodarsky, G.B., Kurth, W.S., Gurnett, D.A., 2001. Ulysses and Cassini at Jupiter: Comparison of the quasiperiodic bursts. In: Rucker, H.O., Kaiser, M.L., Leblanc, Y. (Eds.), Planetary Radio Astronomy V, Proc. of the Fifth International Workshop. Austrian Academy of Sciences Press, Vienna, pp. 41–48.

Kanekal, S.G., Baker, D.N., Blake, J.B., Looper, M.D., Lopate, C.A., 2003. Modulations of jovian electrons at 1 AU during solar cycles 22–23. Geophys. Res. Lett. 30, doi:10.1029/2003GL017502.

Krimigis, S.K., Mitchell, D.G., Hamilton, D.C., Dandouras, J., Armstrong, T.P., Bolton, S.J., Cheng, A.F., Gloeckler, G., Hsieh, K.C., Keath, E.P., Krupp, N., Lagg, A., Lanzerotti, L.J., Livi, S., Mauk, B.H., McEntire, R.W., Roelof, E.C., Wilken, B., Williams, D.J., 2002. A nebula of gases from Io surrounding Jupiter. Nature 415, 994–996.

Krupp, N., Woch, J., Lagg, A., Espinosa, S.A., Livi, S., Krimigis, S.M., Mitchell, D.G., Williams, D.J., Cheng, A.F., Mauk, B.H., McEntire, R.W., Armstrong, T.P., Hamilton, D.C., Gloeckler, G., Dandouras, J., Lanzerotti, L.J., 2002. Leakage of energetic particles from Jupiter's dusk magnetosphere: Dual spacecraft observations. Geophys. Res. Lett. 29, doi:10.1029/2001GL014290.

Krupp, N., Woch, J., Lagg, A., Livi, S., Mitchell, D.G., Krimigis, S.M., Dougherty, M.K., Hanlon, P.G., Armstrong, T.P., Espinosa, S.A., 2004. Energetic particle measurements in the vicinity of Jupiter: Cassini MIMI/LEMMS results. J. Geophys. Res. 109, doi:10.1029/2003JA010111.

Kurth, W.S., Gurnett, D.A., Scarf, F.L., 1989. Jovian type III bursts. J. Geophys. Res. 94, 6917–6924.

Kurth, W.S., Gurnett, D.A., Hospodarsky, G.B., Farrell, W.M., Roux, A., Dougherty, M.K., Joy, S.P., Kivelson, M.G., Walker, R.J., Crary, F.J., Alexander, C.J., 2002. The dusk flank of Jupiter's magnetosphere. Nature 415, 991–994.

Ladreiter, H.P., 1991. The cyclotron maser instability—Application to low-density magnetoplasmas. Astrophys. J. 370, 419–426.

Ladreiter, H.P., Leblanc, Y., 1989. Jovian hectometric radiation: Beaming, source extension, and solar wind control. Astron. Astrophys. 226, 297–310.

MacDowall, R.J., Kaiser, M.L., Desch, M.D., Farrell, W.M., Hess, R.A., Stone, R.G., 1993. Quasiperiodic jovian radio bursts: Observations from the Ulysses radio and plasma wave experiment. Planet. Space Sci. 41, 1057–1072.

Matson, D.L., Spilker, L.J., Lebreton, J.-P., 2002. The Cassini/Huygens mission to the saturnian system. Space Sci. Rev. 104, 1–58.

Mauk, B.H., Clarke, J.T., Grodent, D., Waite Jr., J.H., Paranicas, C.P., Williams, D.J., 2002. Transient aurora on Jupiter from injections of magnetospheric electrons. Nature 415, 1003–1004.

McKibben, R.B., Simpson, J.A., Zhang, M., 1993. Impulsive bursts of relativistic electrons discovered during Ulysses' traversal of Jupiter's duskside magnetosphere. Planet. Space Sci. 41, 1041–1058.

Morioka, A., Tsuchiya, F., 1996. Solar wind control of jovian electron flux: Pioneer 11 analysis. Geophys. Res. Lett. 23, 2963–2966.

Pallier, L., Prange, R., 2001. More about the structure of the high-latitude jovian aurorae. Planet. Space Sci. 49, 1159–1173.

Pallier, L., Prange, R., 2004. Detection of the southern counterpart of the jovian northern polar cusp: Shared properties. Geophys. Res. Lett. 31, doi:10.1029/2003GL018041.

Prange, R., Zarka, P., Ballester, G.E., Livengood, T.A., Denis, L., Carr, T., Reyes, F., Bame, S.J., Moos, H.W., 1993. Correlated variations of UV and radio emissions during an outstanding jovian auroral event. J. Geophys. Res. 98, 18779–18792.

Prangé, R., Chagnon, G., Kivelson, M.G., Livengood, T.A., Kurth, W.S., 2001. Temporal monitoring of Jupiter's auroral activity with IUE during the Galileo mission—Implications for magnetospheric processes. Planet. Space Sci. 49, 405–415.

Prange, R., Pallier, L., Hansen, K.C., Howard, R., Vourlidas, A., Courtin, R., Parkinson, C., 2004. A CME-driven interplanetary shock traced from the Sun to Saturn by planetary auroral storms. Nature 432, 78–81.

Pryor, W.R., Stewart, A.I.F., Simmons, K.E., Ajello, J.M., Tobiska, W.K., Clarke, J.T., Gladstone, G.R., 2001. Detection of rapidly varying H_2 emissions in Jupiter's aurora from the Galileo orbiter. Icarus 151, 314–317.

Southwood, D.J., Kivelson, M.G., 2001. A new perspective concerning the influence of the solar wind on the jovian magnetosphere. J. Geophys. Res. 106, 6123–6130.

Steffl, A.J., Stewart, A.I.F., Bagenal, F., 2004a. Cassini UVIS observations of the Io plasma torus. I. Initial results. Icarus 172, 78–90.

Steffl, A.J., Bagenal, F., Stewart, A.I.F., 2004b. Cassini UVIS observations of the Io plasma torus. II. Radial variations. Icarus 172, 91–103.

Stone, R.G., Bougeret, J.L., Caldwell, J., Canu, P., de Conchy, Y., Cornilleau-Wehrlin, N., Desch, M.D., Fainberg, J., Goetz, K., Goldstein, M.L., Harvey, C.C., Hoang, S., Howard, R., Kaiser, M.L., Kellogg, P.J., Klein, B., Knoll, R., Lecacheux, A., Lengyel-Frey, D., MacDowall, R.J., Manning, R., Meetre, C.A., Meyer, A., Monge, N., Monson, S., Nicol, G., Reiner, M.J., Steinberg, J.L., Torres, E., de Villedary, C., Wouters, F., Zarka, P., 1992. The unified radio and plasma wave investigation. Astron. Astrophys. Suppl. Ser. 92, 291–316.

Tsurutani, B.T., Arballo, J.K., Galvan, C., Zhang, L.D., Zhou, X.-Y., Lakhina, G.S., Hada, T., Pickett, J.S., Gurnett, D.A., 2002. Polar cap boundary layer waves: An auroral zone phenomena. J. Geophys. Res. 106, 19035–19055.

Vasavada, A.R., Bouchez, A.H., Ingersoll, A.P., Little, B., Anger, C.D., the Galileo SSI Team, 1999. Jupiter's visible aurora and Io footprint. J. Geophys. Res. 104, 27133–27142.

Waite, J.H., Gladstone, G.R., Lewis, W.S., Goldstein, R., McComas, D.J., Riley, P., Walker, R.J., Robertson, P., Desai, S., Clarke, J.T., Young, D.T., 2001. An auroral flare at Jupiter. Nature 410, 787–789.

Williams, D.J., McEntire, R.W., Jaskulek, S., Wilken, B., 1992. The Galileo energetic particles detector. Space Sci. Rev. 60, 385–412.

Woch, J., Krupp, N., Lagg, A., 2002. Particle bursts in the jovian magnetosphere: Evidence for a near-Jupiter neutral line. Geophys. Res. Lett. 29, doi:10.1029/2001GL014080.

Young, D.T., 57 colleagues, 2004. Cassini plasma spectrometer investigation. Space Sci. Rev. 114, 1–112.

Zhang, M., Simpson, J.A., McKibben, R.B., 1993. Relativistic electron flux anisotropies in the duskside jovian magnetosphere: A test for source location and escape mechanism. Planet. Space Sci. 41, 1029–1040.

Zhou, X., Tsurutani, B.T., 1999. Rapid intensification and propagation of the dayside aurora: Large-scale interplanetary pressure pulses (fast shocks). Geophys. Res. Lett. 26, 1097–1100.

Zhou, X., Tsurutani, B.T., 2001. Interplanetary shock triggering of nightside geomagnetic activity: Substorms, pseudobreakups, and quiescent events. J. Geophys. Res. 106, 18957–18968.